Nonlinear System Identification of a Homogeneous Charge Compression Ignition Engine

T. Mottin * **E. Oroski** ** **Carlos, T. M.** *** **Silveira, L. B.** **** **Velásquez Alegre, J. A. A** †

* *Federal University of Technology – Paraná (UTFPR) Av. Sete de Setembro, 3165 - Rebouças Curitiba - PR, 80230-901, Brazil (e-mail: mottin@alunos.utfpr.edu.br).*
** *(e-mail: oroski@utfpr.edu.br)*
*** *(e-mail: thiago_morais_carlos@outlook.com)*
**** *(e-mail: lucasbaechtold@alunos.utfpr.edu.br)*
† *(e-mail: velasquez@utfpr.edu.br)*

Abstract: The primary aim of this study was to develop a comprehensive multi-variable model for Homogeneous Charge Compression Ignition (HCCI) engines and evaluate its efficacy by comparing it to simulated HCCI engine data. The complexity of the engine's nonlinear dynamics necessitated the development of appropriate models to address the associated control challenges. Multiple Inputs Single Output (MISO) models were employed to capture the pressure and temperature variables. The estimated outputs were generated using Nonlinear Autoregressive with Exogenous Inputs (NARX) and Hammerstein-Wiener (HW) models, both were used as black box models. The performance of each model was assessed using metrics such as Normalized Root Mean Square Error (NRMSE), Mean Square Error (MSE), and Akaike's Final Prediction Error (FPE). The results highlight the effectiveness of the Hammerstein-Wiener models in accurately representing the intricate dynamics of complex combustion, as observed in HCCI engines. The consistency of these models in delivering reliable outcomes further underscores their suitability for modeling such intricate systems.

Keywords: HCCI Engines, System Identification, NARX models, Wavelet Networks, Hammerstein-Wiener models.

1. INTRODUCTION

Automotive and transport sectors are crucial for improving people's quality of life and promoting economic growth (Levin, 2019). The United Nations has identified sustainable transportation as a key goal to achieve by 2030, with a focus on safety, accessibility, and reduced CO_2 [1] emissions (Sachs et al., 2022). Electric vehicles are a proposed solution to achieving these goals, however, their adoption faces social, cultural, and technological barriers, particularly in countries like Brazil, which require significant investment in infrastructure and production line modifications due to the predominance of internal combustion engines (Silva and Pizzolato, 2022).

Homogeneous Charge Compression Ingition (HCCI) engines combine features of spark ignition and diesel engines, with premixed fuel-air ratios and automatic combustion, resulting in increased efficiency and reduced emissions of NO_x [2] when compared to Spark Ignitions (SI) and diesel engines (Wu et al., 2018). In line with this objective, the paper presents a comprehensive study focused on the modeling and identification of a flex-fuel HCCI engine. The methodology employed in this research involves system identification based on numerical simulation. The primary aim is to develop a robust multi-variable model using Multiple Inputs Multiple Outputs (MIMO) approach. This MIMO model is generated by integrating and analyzing two distinct Multiple Inputs Single Output (MISO) models. Furthermore, the models are rigorously compared using measurable metrics to assess their performance and effectiveness.

The development of flex-fuel engines that incorporate homogeneous charge compression ignition (HCCI) technology represents a potential solution for sustainable transportation, as it enables a more optimized internal combustion process compared to traditional engine ignition (Janakiraman et al., 2013). However, there are several challenges associated with the adoption of HCCI technology over traditional Spark Ignition (SI) and Compression Ignition (CI) engines. The use of compatible fuel is crucial to the development of this engine, as lean mixtures allow for optimized compression ratios, resulting in high thermal efficiency (Janakiraman et al., 2013). Nevertheless, due to the specific combustion conditions required, a high degree of robust control, modeling, and data validation is nec-

* The authors express their gratitude to the Rota 2030 Program for the support provided through the Research Development Foundation - Fundep (Rota 2030/Linha V Project/Process 27192*45).

[1] *CO_2: Carbon dioxide

[2] *NO_x: Nitrogen Oxides

essary for each parameter to ensure optimal combustion (Janakiraman et al., 2013).

In order to address the modeling and control problem of HCCI engine, Janakiraman et al. (2013) applied neural networks and principal component analysis (PCA) for the identification of an HCCI engine. In this work, it was developed an HCCI engine identification framework using multiple neural network models, including MLP and RBN, coupled with PCA to improve efficiency and accuracy.

According to Shaver et al. (2009), a physics-based model was developed to account for the effects of residual gases on the combustion process and capture the dynamic behavior of HCCI engines. The authors highlighted the challenges associated with modeling HCCI engines in the presence of residual gases, which can significantly affect the combustion phasing. This work has presented a novel model-based approach that addresses the control challenges through the utilization of nonlinear Model Predictive Control (MPC). Its purpose was to control the temperature of the incoming air and the amount of residual gas, with the objective of attaining the desired timing of combustion. The control strategy takes into account the nonlinearities of the system and generates optimal control actions to achieve the desired combustion phasing.

The control of combustion process with a lean air-fuel mixture and combustion phasing control was investigated by Bengtsson et al. (2004). In this work It was used a six-cylinder heavy-duty engine model, and proposed the use of nonlinear control strategies such as model predictive control and a Model-based control, which were estimated using system identification.

In the study conducted by Janakiraman et al. (2013), Neural Networks were utilized to address the HCCI engine identification problem and develop their models. However, this research did not consider the effects of temperature on the engine, which can directly impact the accuracy of their models. This omission was pointed out by Bengtsson et al. (2004) and Shaver et al. (2009), whom focused on physics-based models, this work may have limited the model's efficiency compared to a more flexible black box model. Furthermore, the issue of system nonlinearities was not discussed in (Bengtsson et al., 2004), which can significantly affect the model's efficiency if an inappropriate model is chosen. These gaps need to be addressed to improve the accuracy and effectiveness of HCCI engine modeling and control. Consequently, this paper serves as a complementary contribution to existing research. It introduces a black box Hammerstein-Wiener model for temperature and pressure, allowing for the observation and identification of nonlinearities in the input and output variables of the HCCI engine.

The paper is structured as follows: Section 2 discusses the HCCI system, while Section 3 covers the modelling and system identification. Methodology steps are discussed in Section 4. Results and conclusions are presented in Sections 5 and 6, respectively.

2. HCCI ENGINE

The combustion process in HCCI engines is not controlled by a specific mechanism. Instead, it is determined by the charge compression within the cylinder chamber and is also influenced by the combustion conditions of the fuel being used (Coskun et al., 2018). At first, the major difference between an HCCI and a conventional engine is the way that internal combustion occurs. HCCI engine do not have a spark as a trigger for ignition, so their combustion is going to be correlated to the gas mixture properties, which increase several phenomena such chemical kinetics, heat transfer, gas transport and mixing (Janakiraman et al., 2013). Air-fuel mixture is premixed in a pre oxidation step, and inside the combustion chamber this engine operates with homogeneous charge compression, which allow that internal combustion occurs simultaneously in many points of this chamber and increase its efficiency (Wu et al., 2018). Another system that contribute to a better combustion in HCCI engines is the Exhaust Gas Recirculation (EGR). This system is responsible to reduce the exhaust emissions barely to zero emission. It incorporates a functional mechanism that connects the exhaust gas flow section to the intake system, leading to an impoverishment of the air-fuel mixture. This condition is unfavorable for the generation of NO_x and smoke (Abd-Alla, 2002). An HCCI single cylinder schematic is shown in Fig.1, where one can see:

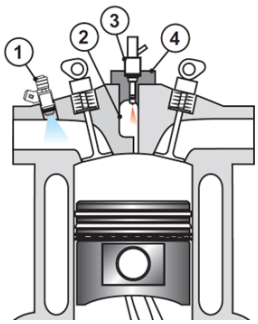

Fig. 1. Single cylinder HCCI schematic.

- (1) Low pressure injector;
- (2) Pre oxidation chamber;
- (3) High pressure injector;
- (4) Compression ratio adjustment shim.

In summary, the high-pressure injector (3) is activated and injects a slightly "lean" mixture into the pre-oxidation chamber (2). This mixture is then subjected to high temperatures and pressures, promoting pre-oxidation to a degree sufficient to advance the combustion of hydrated ethanol to the same level as gasoline (Hunicz et al., 2020). Subsequently, the intake valve is opened, and the controlled mixture of air and fuel, exiting from the low-pressure injector (1), enters the combustion chamber. Additionally, to accommodate the need for varying the volume of the pre-chamber in order to achieve an optimal compression ratio, there is a partition (4) to facilitate this adjustment. Given the need to adjust the properties of the mixture cycle by cycle, so that combustion occurs at the right timing, a control model that describes the relationship between various variables and engine performance is necessary. It is essential to use system identification to obtain such a model. This modelling methodology are presented in the next section.

3. MODELLING AND SYSTEM IDENTIFICATION

System identification is the knowledge area whose objective is to construct and implement mathematical models to dynamical systems, with narrow previous knowledge about this system (AGUIRRE, 2007).

3.1 Black box model

A black box model is a simplified representation of a system that focuses on its inputs and outputs without explicitly incorporating the physical parameters or equations associated with that system. Instead, the parameters are treated as adjustable factors used to optimize the model's fit to the observed data. (LJUNG, 1999).

One of the black box model characteristics is that, they require minimal prior knowledge of the system being modeled (AGUIRRE, 2007). This can be an advantage in practical experiments where complete information may not be available.

3.2 Model Structure

Since HCCI is considered a nonlinear system (Bengtsson et al., 2004), this section begins by defining the nonlinear models employed in this paper. These models are Hammerstein-Wiener and Nonlinear AutoRegressive with eXogeneous input (NARX).

3.3 Hammerstein and Wiener Models

Selecting a mathematical representation in a black-box model is difficult, particularly in nonlinear models where there are many possible representations (Ljung, 2001). One alternative is to combine multiple linear dynamic models for each small range of the system (AGUIRRE, 2007). In this context, Hammerstein and Wiener models are a combination of a Static Model (SM) in cascade with a Linear Dynamic Model (LDM) (Alqahtani et al., 2016). The Hammerstein model, shown in Fig. 2 (a), uses the SM, $f_H(.) : \mathbb{R} \to \mathbb{R}$, and the LDM, $G(q, \theta)$, to represent the nonlinearity. On the other hand, Wiener models, mostly used to represent the nonlinearity of the output, combine the LDM, $G(q, \theta)$, with the SM, expressed as $f_W(.) : \mathbb{R} \to \mathbb{R}$, as illustrated in Fig. 2 (b).

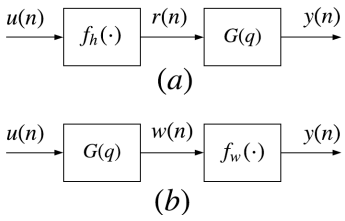

Fig. 2. (a) Representation of a Hammerstein model: composed of a nonlinear static function: $f_H(.)$, and a linear dynamic block: $G(q)$; (b) Representation of a Wiener model: composed of LDM: $G(q)$, and a SM: $f_H(.)$.

In principle, it is feasible to model a nonlinear system by employing a Linear Dynamic Model (LDM) between two Static Models (SMs) to capture the nonlinearities present in the system. This approach is commonly referred to as the Hammerstein-Wiener (HW) model (Alqahtani et al., 2016). The HW model, outlined in (1) and depicted in Fig. 3, exemplifies this concept.

$$\begin{aligned} r(n) &= f_H(u(n)), \\ w(n) &= G(q,\theta)r(n), \\ y(n) &= f_W(G(q,\theta)r(n)), \\ y(n) &= f_W(G(q,\theta)f_H(u(n))). \end{aligned} \tag{1}$$

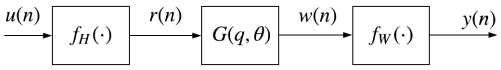

Fig. 3. Hammerstein-Wiener representation. This figure illustrates the Linear Dynamic Model in $G(q, \theta)$, where $f_H(\cdot)$ and $f_W(\cdot)$ represent the input and output nonlinear functions, respectively.

If the transfer function is represented as a polynomial of regressors as the other models presented, we can define the input and outputs of each block as presented in Fig. 3. The resulting equation for $H(q)$ can be described as

$$w(n) = \frac{B(q)}{F(q)} r(n), \tag{2}$$

where $F(q) \in \mathbb{R}^{N_u}$ is the delay operator applied to the inputs $r(n) \in \mathbb{R}^{N_u}$ of the linear system, $w(n) \in \mathbb{R}^{N_y}$ is the output of the linear system, $r(n) \in \mathbb{R}^{N_u}$ is the input vector after applying the static nonlinear function.

The static nonlinear blocks are represented by $f_W(.)$ and $f_H(.)$ in the Hammerstein-Wiener (HW) model, with a focus on the Piecewise Linear function (PWL) used in this work (Tao and Tian, 1998). The PWL represents a nonlinear function combining linear functions in specific intervals (Ljung, 2001). A MISO model is then illustrated in Fig. 4, with multiples HW models added together to obtain the output.

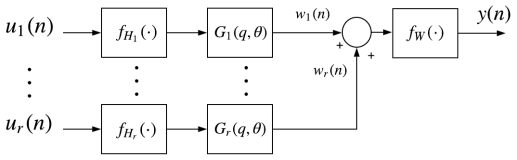

Fig. 4. Hammerstein-Wiener MISO representation. Where $u_1, \ldots, u_r$ represent the r inputs of the MISO system and $f_W(\cdot)$ is the output nonlinear function.

For temperature and pressure Hammerstein-wiener models are expressed as (5)

$$y(n) = f_W(w(n)), \tag{3}$$

$$\omega(n) = \sum_{i=1}^{r} \omega_i(n), \tag{4}$$

$$\omega_i(n) = fh_i(u_i(n))Gi(q,\theta), \tag{5}$$

where $\omega_i(n)$ is the model output, f_{h_i} represents the nonlinear function, i is the index, $G_i(q, \theta)$ is the LDM, and

$u_i(n)$ are the inputs varying from $h_i = 1$ to r, where r is the number of inputs.

The type of nonlinear function explored in this paper for $f_i(\cdot)$ and $f_o(\cdot)$ is the piecewise linear (PWL). This type of function can be represented in the following way:

$$f(u) = \begin{cases} m_{R1}u, & if \quad 0 \leq u \leq u_{R1}, \\ m_{R2}(u - u_{R1}) + m_{R1}u_{R1}, & if \quad u > u_{R1}, \\ m_{L1}u, & if \quad u_{L1} \leq u < 0, \\ m_{L2}(u - u_{L1}) + m_{L1}u_{L1}, & if \quad u < u_{L1}, \end{cases} \tag{6}$$

in which m_{L2}, m_{L1}, m_{R1} and m_{R2} are the slopes of the linear segments, u_{L1} is a constant for negative inputs and u_{R1} is a constant for positive inputs (Tao and Tian, 1998). The structure of this nonlinear function can be observed in Fig. 5.

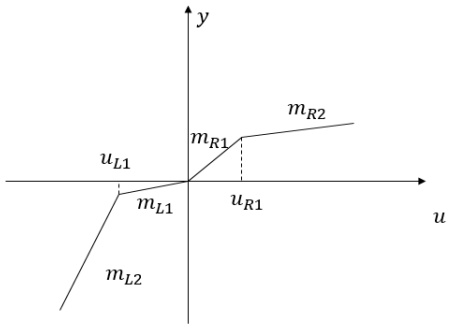

Fig. 5. Example of a piecewise linear function with $(2+2)$ segments.

For further information regarding Hammerstein-Wiener equations, please refer to Nelles and Isermann (1995).

3.4 NARX Models and Walvelet Output Functions

Nonlinearity is a common characteristic found in practical dynamics systems. In certain instances, nonlinear systems can be approximated as linear systems (AGUIRRE, 2007). Nevertheless, for the majority of systems, nonlinear models are required to accurately capture their dynamic behavior (AGUIRRE, 2007). This section specifically emphasizes the utilization of NARX models and their application in capturing the nonlinear characteristics of the HCCI system.

NARX are discrete-time models, that use its previous inputs and outputs signal values (AGUIRRE, 2007). As represented in (7):

$$y(k) = F[y(k-1), \cdots, y(k-(n_y), u(k-\tau_d), \cdots, u(k-n_u)], \tag{7}$$

in this case, $y(k)$ represents the output of the system at time k, where $\mathrm{F}\{\cdot\} : \mathbb{R}^{n_y+n_y-\tau_d+1} \rightarrow \mathbb{R}$ represents the nonlinear function that maps the input and previous outputs to the current output, τ_d is the pure delay between input and output signals, $u(k-n_u)$ and $y(k-n_y)$ are the system's input and output, n_u and n_y time steps ago, respectively Billings (2013).

The model output function involves sending shorter waveforms with high frequencies instead of pulses with the same duration (Mallat, 1999). This paper consider the Discrete Wavelet Transform (DWT) (Nappo, 2013), which are represented as follows:

$$W(m,n) = 2^{(\frac{-m}{2})} \sum_{k=0}^{n-1} f(k)\varphi\left(\frac{k - n2^m}{2^m}\right), \tag{8}$$

being (8), $W(m,n)$ represents the output or the wavelet coefficient at a scale m and position n, $f(k)$ is a function of the input signal at time step k, it is a past value of input signal. In $\varphi\left(\frac{k-n2^m}{2^m}\right)$ this represents the mother wavelet function evaluated at a scaled and shifted argument. The term $\frac{k-n2^m}{2^m}$ indicates the relative position of the $k-th$ input sample, adjusted by n and m. The summation is performed over k from 0 to $n-1$. The term $2^{(-\frac{m}{2})}$ is a scaling factor, affecting the amplitude of the wavelet coefficient. For more information regarding Wavelet, please refer to Mallat (1999).

3.5 Validation Metrics

When quantifying the accuracy of a predictive model, the Mean Square Error (MSE) and Normalized Root Mean Square Error (NRMSE) are used to determine the fitness between the model and collected data (LJUNG, 1999). Besides that, the Aikaike's Final Prediction Error Criterion (FPE) were also used to measure these nonlinear models accuracy, for more details see Niedźwiecki and Ciołek (2017). The FPE equation is presented in (9):

$$FPE = det\left(\frac{1}{N}\sum_{1}^{N} e(t,\hat{\Theta}_N)(e(t,\hat{\Theta}_N))^T\right)\left[\frac{1+\frac{d}{N}}{1-\frac{d}{N}}\right], \tag{9}$$

where, N is the number of values in the estimation data vector, $e(t)$ is the prediction errors vector, Θ_N represents the estimated parameters and d is the number of estimated parameters.

$$MSE = \frac{1}{N}\sum_{k=0}^{N-1}\left[p(k) - \hat{p}(k)\right]^2, \tag{10}$$

$$NRMSE = \left[1 - \sqrt{\frac{(\sum_{k=0}^{n-1}(p(k) - \hat{p}(k))^2}{(\sum_{k=0}^{n-1}(p(k) - \hat{p})^2}}\right]100\%, \tag{11}$$

considering

$$\hat{p} = \frac{1}{N}\sum_{k=0}^{N-1} p(k), \tag{12}$$

where $\hat{p}$ is the estimated output from the system, *p(k)* represents the actual value of the variable and N is the number of sample, k is the estimation variable, which varies from 0 to N-1.

In this context, the next section will present the methodology employed in this research.

4. METHODOLOGY

This section describes the key considerations that guided the research process, with a focus on the use of HCCI model data as the foundation for the study.

A simulated single cylinder engine model was used to generate the data, with the structure presented by Velásquez and Milanez (1996); Och et al. (2013), considered this engine powered with ethanol. Based on the simulated data, certain variables were utilized to understand how the system acts when subjected to those input and output

variables. Afterwards, using the Sample Time (Ts) equal 1.9200×10^{-5} Seconds (s), two models were generated for pressure and temperature. The purpose of this investigation is to decrease the computational expenses and intricacy of the simulated model, developed in the research conducted by Velásquez and Milanez (1996); Och et al. (2013).

The data produced by Velásquez and Milanez (1996); Och et al. (2013) comprises 34,000 cycles of the simulated HCCI engine. For the models formulated in this paper, 70% of this data was allocated for training and testing purposes, while the remaining 30% was reserved for validation.

Input variables are described as follows:

- Crank angle: it refers to the angular position of the crankshaft of an engine and is measured in degrees [°];
- Mass fuel injected: represents the mass of fuel injected in the cylinder chamber and is measured in kilograms $[kg]$;
- Injection rate: this variable brings the injection rate in kilograms per seconds $[kg/s]$.

Taking into account the input variables presented above, two MISO models were generated.

The model for temperature and pressure displays the variables required to generate output models for the intake temperature and pressure within the cylinder chamber, as illustrated in Fig. 6. Pressure model were generated

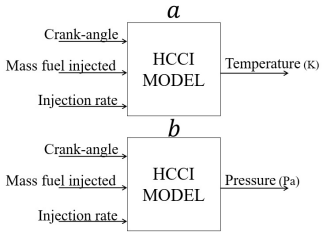

Fig. 6. Multiple Inputs Single Output (MISO) for temperature nonlinear model inputs and outputs a and pressure nonlinear model inputs and outputs b variables of an HCCI engine generated from simulated data.

considering a nonlinear function Wavelet Network (WN) as shown in (8). It is known as a DWT function and was used as the output function model. Its results are shown in Section 5.

The engine specifications considered in this simulation are presented in Table 1.

Table 1. Engine specifications

Engine type	HCCI
N° of cylinders	1
Fuel	Ethanol
Cylinder diameter	71 mm
Piston stroke	84 mm
N° of admission valves	2
N° of exhaust valves	2

The configurations of the Hammerstein, Wiener, and Hammerstein-Wiener models are detailed in Table 2 and Table 3 for temperature and pressure, respectively. In these tables, PWL In and PWL Out represent the number of linear segments for inputs and outputs, respectively. The input delay is presented in the fifth column. The metric results are presented in Tables 4 and 5 for temperature and pressure, respectively.

Table 2. Configuration of simulated temperature Hammerstein-Wiener models.

Model	PWL In	Zeros	Poles	Delay	PWL Out
H10T	10/10/10	2	3	1	0
WNER10T	0	2	4	1	10
HW40T	40/40/40	6	6	2	40

Table 3. Configuration of simulated pressure Hammerstein-Wiener models.

Model	PWL In	Zeros	Poles	Delay	PWL Out
H20P	20/10/20	2	3	1	0
HW20P	20/10/10	2	3	1	20
WNER30P	0	2	3	1	30

Using these models, it becomes feasible to analyze the relationship between input and output variables. It leads to the identification of an output model that conforms to the engine data and meets the desired metric adopted in this paper MSE, NRMSE and FPE.

5. RESULTS

The models selected in this paper were developed using the methodology presented in Section 4. The results obtained were represented as MISO models with inputs and outputs shown in Fig. 6.

The best model structures for temperature and pressure were obtained using Hammerstein-Wiener models with Piecewise Linear (PWL) functions as inputs (PWL In) and outputs (PWL Out) nonlinearities. For temperature, the Hammerstein-Wiener function (HW40T) was divided into 40 linear segments for both inputs and outputs. Regarding pressure, the optimal function structure for Hammerstein-Wiener (HW20P) consisted of dividing it into 20, 10, and 10 linear segments for inputs, respectively, and 20 linear segments for the output. For NARX pressure model, the nonlinear function were implemented using the wavelet networks.

In the case of the Hammerstein models for temperature (H10T) and pressure (H20P), they were also divided into input and output PWL nonlinearities. H10T had 10 linear segments for inputs and no linear segments for the output, while H20P consisted of 20, 10, and 20 linear segments for inputs, respectively, and no one for the output.

In the Wiener models generated, the best results were achieved using PWL functions for both inputs and output for temperature (WNER10T) and pressure (WNER30P) models. Specifically, WNER10T had one linear segment for inputs and 10 linear segments for the output, whereas WNER30P had one linear segment for input and 20 linear segments for the output.

The figures 7, 8 and 9 indicate that Hammerstein-Wiener models are better suited for representing the dynamics of the HCCI engine, specifically for temperature and pressure variables. Tables 4 and 5 present the accuracy

of the temperature and pressure models, respectively, using metrics such as NRMSE, MSE, and FPE. These metrics were employed to determine which classes of models exhibit the closest adherence to the dataset.

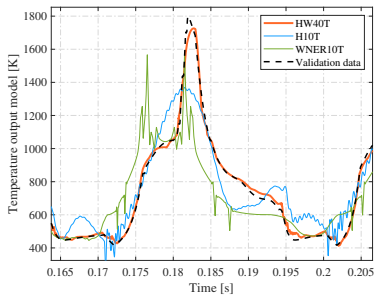

Fig. 7. Temperature output model. Comparison of Hammerstein-Wiener model accuracy. HW40T exhibited the best accuracy and adherence to model dynamics, with NRMSE = 87.76%, MSE = 1.611×10^1, and FPE = 1.610×10^1.

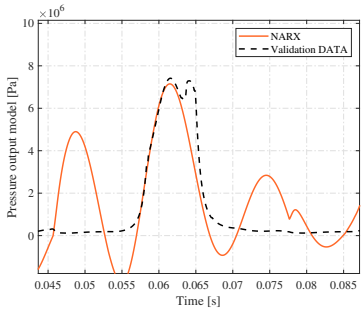

Fig. 8. First pressure model output analysis. Comparing NARX and model output. NARX presented bad dynamics representation. NARX model presented NRMSE = 39.52%, MSE = 2.608×10^{12} and FPE = 6.505×10^7.

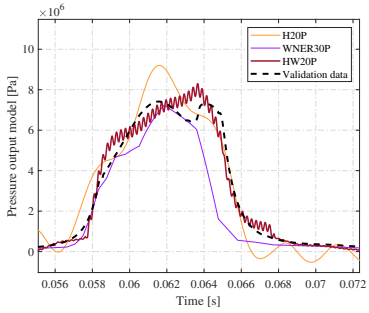

Fig. 9. Pressure model output comparing best results: Hammerstein-Wiener models followed the system dynamics. HW20P presented NRMSE = 88.52%, MSE = 1.61×10^{11} and FPE = 1.629×10^{11}.

Table 4. Fitness of the simulated temperature output model.

Model	NRMSE	MSE	FPE
H10T	53.49%	2.327×10^4	2.342×10^4
WNER10T	45.82%	1.264×10^4	1.292×10^4
HW40T	**87.76%**	1.611×10^1	1.610×10^1

Table 5. Simulated pressure output model's fitness.

Model	NRMSE	MSE	FPE
NARX	**39.52%**	2.608×10^{12}	6.505×10^7
H20P	77.50%	3.87×10^{11}	3.907×10^{11}
HW20P	**88.52%**	1.61×10^{11}	1.629×10^{11}
WNER30P	49.66%	1.935×10^{12}	1.947×10^{12}

The Hammerstein-Wiener models presented the best results for temperature and pressure models. For pressure, when comparing the NRMSE of its best HW model (HW20P) with NARX model there is a difference of approximately 49% and comparing to Hammerstein (H20P) model the difference is of 11,02%. In temperature, HW model (HW40T) NRMSE showed to be approximately 34.27% more efficient than Hammerstein (H10T) model, which presented an NRMSE of 53.49% and its difference for the Wiener model (WNER10T) is approximately 41,94%. In order to accomplish the HCCI engine modelling, Hammerstein and Wiener was one of the methods used for pressure and temperature models. With these models, the variables for input and output were capable of being analyzed for nonlinearities.

Using the notation described in section 4 in (2), the nonlinear functions for the Hammerstein-Wiener model with the best fit can be seen in Fig. 7 and Fig. 9. The resulting equations for pressure $F_P(q)$ and $B_P(q)$ are presented in (13) to (18).

$$F_{P_1(q)} = 1 - 2.697\ q^{-1} + 2.651\ q^{-2} + 0.940\ q^{-3}, \quad (13)$$

$$F_{P_2(q)} = 1 - 2.997\ q^{-1} + 2.996\ q^{-2} - 0.999\ q^{-3}, \quad (14)$$

$$F_{P_3(q)} = 1 - 0.999\ q^{-1} + 0.999\ q^{-2} + 0.999\ q^{-3}, \quad (15)$$

$$B_{P_1(q)} = 4.743\ q^{-1} + \ q^{-2}, \quad (16)$$

$$B_{P_2(q)} = q^{-1} - 0.999\ q^{-2}, \quad (17)$$

$$B_{P_3(q)} = q^{-1} - 0.610\ q^{-2}. \quad (18)$$

The resulting equations for temperature $FT(q)$ and $BT(q)$ are presented in (20) to (25).

$$F_{T_1(q)} = 1 - 1.254\ q^{-1} - 0.852\ q^{-2} + 0.494\ q^{-3} + 0.494q^{-4} - 0.236q^{-5} - 0.368\ q^{-6}, \quad (19)$$

$$F_{T_2(q)} = 1 - 4.289\ q^{-1} + 7.001\ q^{-2} - 4.848\ q^{-3} + 0.437\ q^{-4} + 1.110\ q^{-5} - 0.411\ q^{-6}, \quad (20)$$

$$F_{T_3(q)} = 1 - 2.930\ q^{-1} + 2.852\ q^{-2} - 0.095\ q^{-3} - 2.509\ q^{-4} + 2.546\ q^{-5} - 0.864\ q^{-6}, \quad (21)$$

$$B_{T_1(q)} = -0.480\ q^{-1} - \ q^{-2} - 0.332\ q^{-3} - 0.241\ q^{-4} - 0.117\ q^{-5}0.171\ q^{-5}, \quad (22)$$

$$B_{T_2(q)} = 0.261\ q^{-1} - 0.664\ q^{-2} + 0.456\ q^{-3} + 1.034\ q^{-4} - 2.086\ q^{-5} + \ q^{-6}, \quad (23)$$

$$B_{T_3(q)} = 0.210\ q^{-1} - 0.710\ q^{-2} + \ q^{-3} \qquad (24)$$
$$-0.482\ q^{-4} - 0.311\ q^{-5} + 0.293\ q^{-5}.$$

The crank angle nonlinearity for temperature and pressure are respectively shown in Fig.10.

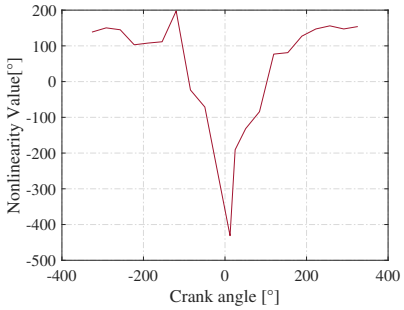

Fig. 10. crank angle nonlinearity. This input nonlinearity were generated based on HW models.

The injection rate nonlinearities are presented in Fig. 11. These variables exhibited nonlinearity, however, it does not exhibit as much nonlinearity as the mass of fuel injected into the cylinder chamber for both models.

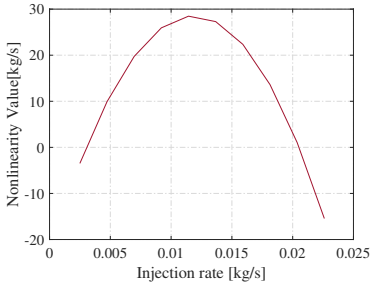

Fig. 11. Injection rate nonlinearity. Generated from HW models. For the pressure model, it was observed that the injection rate input exhibits nonlinearity.

The mass of fuel injected nonlinearities are depicted in Fig. 12. Consequently, the outputs of these models vary in

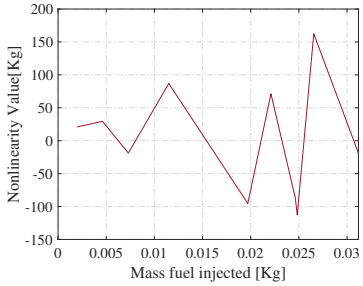

Fig. 12. Mass fuel injected nonlinearity. The mass of fuel injected into the cylinder chamber in the pressure model exhibits nonlinearity and varies in a nonlinear manner. Nonlinearity observed in HW models.

a nonlinear manner, as it is illustrated in Fig. 13 and Fig. 14.

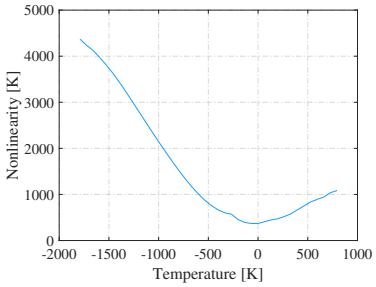

Fig. 13. Temperature output nonlinearity. It shows the nonlinear way that the temperature output varies, based on HW models.

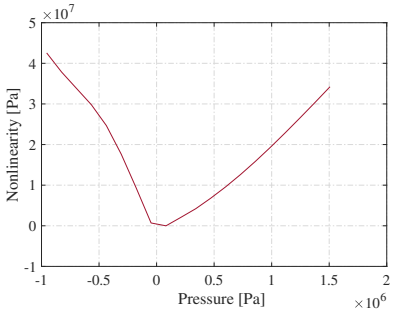

Fig. 14. Pressure output nonlinearities. The nonlinearity in the output dynamics of pressure has been observed, which further emphasizes the need for nonlinear modeling results.

It shows significant nonlinearity not only in the temperature model but also in the pressure model.

6. CONCLUSIONS

In this work, the researchers applied Hammerstein-Wiener and NARX models to assess the temperature and pressure profiles of an HCCI engine - NARX for pressure and Hammerstein-Wiener for both variables. The performance of these models were evaluated using several metrics, including NRMSE (Normalized Root Mean Square Error), MSE (Mean Square Error), and FPE (Final Prediction Error). These metrics are commonly used to quantify the accuracy and predictive capabilities of models. By utilizing these evaluation criteria, the researchers were able to assess and compare the performance of the Hammerstein-Wiener and NARX models in capturing and predicting the temperature and pressure dynamics of the HCCI engine.

The Hammerstein-Wiener model presented an NRMSE of 87.76% for temperature and 88.52% for pressure, while the NARX model achieved an NRMSE of 39.52 % for pressure. These results indicate that the Hammerstein-Wiener models outperformed the NARX model in capturing the dynamics of these variables in the HCCI system, as evidenced by the lower NRMSE values obtained. Specifically, the Hammerstein-Wiener model exhibited an NRMSE approximately 49% higher than the NARX model for pressure. Regarding temperature, the Hammerstein-Wiener model had an NRMSE approximately 34.27% higher than the Hammerstein model. These findings highlight the superiority of the Hammerstein-Wiener models in accurately

modeling the temperature and pressure dynamics of the HCCI system compared to the NARX model. The analysis of the nonlinearities in the Hammerstein-Wiener models revealed that both temperature and pressure in the HCCI system exhibited nonlinearity. This discovery poses significant challenges for controlling the real system. Nonlinearities can make it more difficult to design and implement effective control strategies, as linear control techniques may not be sufficient to handle the complexities introduced by nonlinearity. The presence of nonlinearity suggests that more advanced control methods, such as adaptive or nonlinear control algorithms, may be necessary to accurately control the temperature and pressure dynamics of the HCCI system. The results presented in this work are preliminary. They are going to contribute to implement the control techniques of a HCCI engine prototype. The ongoing development of this prototype is the central focus of this work, with the aim of implementing engine control for this specific design.

In our future work, we aim to explore various types of nonlinear models for describing the dynamic behavior of the HCCI Engine. Specifically, we plan to investigate the applicability of polynomials such as NARMAX and NARMAX-OBF (Orthonormal Basis Functions) models, as well as Neural Networks. Moreover, we intend to validate the performance of Hammerstein-Wiener models using real data obtained from actual HCCI engines. By employing these different modeling approaches and utilizing real-world data, we anticipate gaining valuable insights into the behavior and characteristics of the HCCI Engine.

ACKNOWLEDGEMENTS

The authors express their gratitude to the Rota 2030 Program for the support provided through the Research Development Foundation - Fundep (Rota 2030/Linha V Project/Process 27192*45).

REFERENCES

Abd-Alla, G.H. (2002). Using exhaust gas recirculation in internal combustion engines: a review. *energy conversion and management*, 43(8), 1027–1042.

AGUIRRE, L.A. (2007). *Introdução à Identificação de Sistemas - Técnicas Lineares e Não Lineares Aplicadas à Sistemas Reais*. Editora UFMG, Belo Horizonte MG.

Alqahtani, A., Alsaffar, M., El-Sayed, M., Alajmi, B., et al. (2016). Data-driven photovoltaic system modeling based on nonlinear system identification. *International Journal of Photoenergy*, 2016.

Bengtsson, J., Strandh, F., Johansson, R., Tunestal, P., and Johansson, B. (2004). Control of homogeneous charge compression ignition (hcci) engine dynamics. In *Proceedings of the 2004 American Control Conference*, volume 5, 4048–4053. IEEE.

Billings, S.A. (2013). *Nonlinear system identification: NARMAX methods in the time, frequency, and spatio-temporal domains*. John Wiley & Sons.

Coskun, G., Demir, U., Soyhan, H.S., Turkcan, A., Ozsezen, A.N., and Canakci, M. (2018). An experimental and modeling study to investigate effects of different injection parameters on a direct injection hcci combustion fueled with ethanol–gasoline fuel blends. *Fuel*, 215, 879–891.

Hunicz, J., Mikulski, M., Geca, M.S., and Rybak, A. (2020). An applicable approach to mitigate pressure rise rate in an hcci engine with negative valve overlap. *Applied Energy*, 257, 114018.

Janakiraman, V.M., Nguyen, X., and Assanis, D. (2013). Nonlinear identification of a gasoline hcci engine using neural networks coupled with principal component analysis. *Applied Soft Computing*, 13(5), 2375–2389.

Levin, L. (2019). How may public transport influence the practice of everyday life among younger and older people and how may their practices influence public transport? *Social Sciences*, 8(3). doi:10.3390/socsci8030096. URL `https://www.mdpi.com/2076-0760/8/3/96`.

LJUNG, L. (1999). *System Identification - Theory For The User*. Prentice Hall PTR, Upper Saddle River - New Jersey.

Ljung, L. (2001). Black-box models from input-output measurements. In *IMTC 2001. Proceedings of the 18th IEEE Instrumentation and Measurement Technology Conference. Rediscovering Measurement in the Age of Informatics (Cat. No. 01CH 37188)*, volume 1, 138–146. IEEE.

Mallat, S. (1999). *A wavelet tour of signal processing*. Elsevier.

Nappo, C.J. (2013). *An introduction to atmospheric gravity waves*. Academic press.

Nelles, O. and Isermann, R. (1995). Identification of nonlinear dynamic systems classical methods versus radial basis function networks. In *Proceedings of 1995 American Control Conference-ACC'95*, volume 5, 3786–3790. IEEE.

Niedźwiecki, M. and Ciołek, M. (2017). Akaike's final prediction error criterion revisited. In *2017 40th international conference on telecommunications and signal processing (tsp)*, 237–242. IEEE.

Och, S., Moura, L., Velásquez, J., Lacour, C., Lecordier, B., and Domingues, E. (2013). Experimental and numerical study of admission and exhaust flows in a spark ignition engine. In *European Combustion Meeting*.

Sachs, J., Kroll, C., Lafortune, G., Fuller, G., and Woelm, F. (2022). *Sustainable development report 2022*. Cambridge University Press.

Shaver, G.M., Gerdes, J.C., and Roelle, M.J. (2009). Physics-based modeling and control of residual-affected hcci engines. *Journal of Dynamic Systems, Measurement, and Control*, 131(2).

Silva, A.C.A.C.d. and Pizzolato, N.D. (2022). Using electric vehicles for freight transport purposes and challenges to do an implementation in brazil. *Ambiente & Sociedade*, 25.

Tao, G. and Tian, M. (1998). Discrete-time adaptive control of systems with multisegment piecewise-linear nonlinearities. *IEEE transactions on automatic control*, 43(5), 719–723.

Velásquez, J.A. and Milanez, L.F. (1996). Simulation of admission and exhaust processes in diesel engines. Technical report, SAE Technical Paper.

Wu, Y.Y., Wang, J.H., and Mir, F.M. (2018). Improving the thermal efficiency of the homogeneous charge compression ignition engine by using various combustion patterns. *Energies*, 11(11), 3002.